JOURNAL OF MATERIALS SCIENCE **36** (2001) 5379–5384

Formation of zinc ferrite by solid-state reaction and its characterization by XRD and XPS

S. BERA
Water and Steam Chemistry Laboratory, BARC Facilities, Kalpakkam 603 102, Tamil Nadu, India

A. A. M. PRINCE
Department of Chemistry, Madras Christian College, Tambaram, Chennai 600 059, India

S. VELMURUGAN
Water and Steam Chemistry Laboratory, BARC Facilities, Kalpakkam 603 102, Tamil Nadu, India

P. S. RAGHAVAN, R. GOPALAN
Department of Chemistry, Madras Christian College, Tambaram, Chennai 600 059, India

G. PANNEERSELVAM
Fuel Chemistry Division, IGCAR, Kalpakkam 603 102, Tamil Nadu, India

S. V. NARASIMHAN
Water and Steam Chemistry Laboratory, BARC Facilities, Kalpakkam 603 102, Tamil Nadu, India
E-mail: svn@igcar.ernet.in

A dry mixture of ZnO and α-Fe_2O_3 was annealed at 1200°C; the progress of the formation of the ferrite was monitored by XRD and XPS analyses at different time intervals. The presence of octahedral zinc cation was observed along with the regular tetrahedral Zn in the sample that had undergone 30 minute heat treatment. After three hours of heating, pure normal zinc ferrite was formed. The Zn $2p_{3/2}$ peak binding energy, intensity and line shape were analyzed extensively to show the diffusion of ZnO and the growth of ferrite at different stages of heat treatment. Analysis of the Fe $2p_{3/2}$ line-shape supported the substitution of Fe^{2+} by zinc cations during ferrite formation. The binding energy values of the Zn 2p levels for stoichiometric and non-stoichiometric ferrites were also determined and surface segregation of the zinc was observed by XPS in the non-stoichiometric ferrites.

1. Introduction

Spinels like ferrites and chromites are formed on the steel surfaces used in the fabrication of the coolant system of power reactors. Detailed thermodynamic investigations of transition metal spinel formation revealed that zinc has the highest site preference energy for the tetrahedral site in the spinel structure. So zinc ion in the coolant has been found to be a good candidate to passivate the steel surfaces of the coolant system of Boiling Water Reactors (BWRs) that in turn helped to reduce the radiation field build-up due to radioactive ^{60}Co [1]. The phenomenon of passivation by zinc [2–4] and its role in mitigating the problem of radiation field build-up in water-cooled nuclear reactor are not completely understood. Such surface related phenomenon could be better understood by a detailed study of the materials through surface analytical techniques. XPS has been employed successfully in handling such problems and used extensively for characterisation of Mn, Cr, Ni, Co substituted ferrite [4, 5].

The $Zn_xFe_{3-x}O_4$ spinels adopt normal spinel structure where Zn^{2+} cations occupy the tetrahedral sites irrespective of the value of x. Mössbauer [3, 6] and XRD techniques [7] were employed for the characterization of the ferrites. The random distribution of Zn^{2+} and Fe^{3+} ions among tetrahedral sites was explained using Mössbauer spectroscopy. The effect of temperature on the rate of formation of zinc ferrite was monitored by XRD technique [7, 8]. The mechanism of the zinc ferrite formation is explained [8] as a three-step process, viz: (i) ZnO migrates to the α-Fe_2O_3 grains, due to its higher mobility, (ii) Zn in tetrahedral site of ZnO redistributes itself into the tetrahedral site of spinel in order to form the ferrite at the surface of haematite grains and (iii) the ferrite grain containing Zn diffuses through the ferrite layers towards the haematite lattice [8] for further growth of the ferrite.

In this paper, the results of the detailed XRD and XPS analyses of the $Zn_xFe_{3-x}O_4$ ferrite during its formation by a solid-state reaction are discussed. The line-shape

and intensity of the Zn $2p_{3/2}$ and the Fe $2p_{3/2}$ photoelectron peaks recorded from the ferrites have been used to draw conclusions regarding the formation mechanism of zinc ferrites.

2. Experiment

$ZnFe_2O_4$ was prepared by heating an intimate mixture of ZnO (33.7% by weight) and α-Fe_2O_3 in an aerated atmosphere at 1200°C for 3 hours. The temperature of 1200°C was reached by heating at the rate of 10°C/minute [9] and then cooled to room temperature at the same rate. $Zn_{0.33}Fe_{2.67}O_4$ was prepared by mixing Zn powder (9.3% by weight) and Fe_2O_3 and then heating the mixture to 900°C; the mixture was maintained at this temperature for 20 hours in a flowing argon atmosphere. $Zn_{0.67}Fe_{2.33}O_4$ was prepared by heating ZnO (20.6% by weight), Fe_2O_3 (76.2% by weight) and Fe powder to 900°C and maintaining the mixture at that temperature for 20 hours.

The XRD patterns were recorded at room temperature by using a Philips (XPERT MPD) X-ray diffractometer employing the Cu K_α radiation (40 kV and 45 mA) with 2θ scanning speed of 0.05°/minute and covering the angle range of 10–80°. The XPS measurements were carried out with a VG ESCALAB MkII system using Al-K_α x-ray source and a 150 mm hemispherical analyser with 20 eV pass energy. The binding energy of the XPS system was calibrated by setting Au $4f_{7/2}$ peak at 84.0 eV [10] and was taken as the reference peak for all binding energy measurement. The powder samples were pressed on the indium foil prior to the XPS experiment.

3. Results and discussion

3.1. Study on $ZnFe_2O_4$

The x-ray diffraction patterns for stoichiometric mixture of ZnO and Fe_2O_3, annealed at 1200°C for different time are shown in Fig. 1. In Fig. 1a, a small peak around $2\theta = 35°$ shows the development of spinel phase even at room temperature (marked by *) due to mixing of the powder. Formation of zinc ferrite due to mechanical mixing of ZnO and Fe_2O_3 powders has been observed elsewhere [11] by using XRD. After 30 minutes of heating, development of the peaks corresponding to spinel phase was observed. At this stage the peak corresponding to the presence of a small amount of ZnO was also observed (marked by an arrow in Fig. 1b). The complete formation of zinc ferrite after one hour is indicated by the pattern in Fig. 1c.

Detailed surface studies of the samples were carried out by XPS to check the chemical state of the ferrite formed at different stages of heat treatment. The Zn 2p and Fe 2p photoelectron spectra are shown in Figs 2 and 3 respectively.

In addition to the peak position of the photoelectron spectrum, the full width at half maxima (FWHM) has a direct bearing on the chemical environment and bonding. When two photoelectron peaks are located very near to each other, apparently it gives a broad single peak. In case of Zn, which shows a small shift due to oxidation (~0.3 eV [12]), a very careful observation on

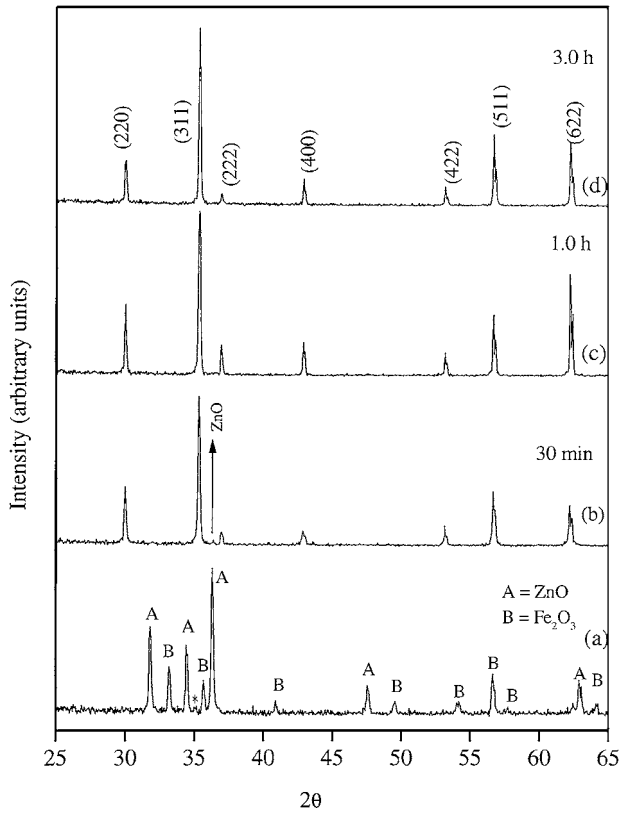

Figure 1 X-ray diffraction pattern for dry mixed ZnO and Fe_2O_3 powder annealed at 1200°C. (a) Physical mixing of powders, (*) indicates the development of spinel. (b) 30 minutes of annealing, (c) 1 hour of annealing and (d) 3 hours of annealing.

the FWHM needs to be made. The satellites, which are the result of the shake-up or shake-off of the valence band electrons, also reflect the chemical environment to some extent. In case of Fe 2p analysis, the background posed a practical problem that limited its peak fitting even when the peaks due to different oxidation states are well separated. In these cases, the satellite peaks were used to derive information regarding the oxidation states.

3.1.1. Zn 2p peak analysis

The Zn $2p_{3/2}$ photoelectron peak for the physical mixture of ZnO and α-Fe_2O_3 before heating was observed at 1021.7 eV that matches well with the literature value corresponding to ZnO [11]. A shoulder at higher binding energy was seen due to the mechanically formed disordered zinc ferrite [13]. The XPS signal shown in Fig. 2a is resolved into two peaks. The peak with the high binding energy corresponds to the mechanically formed zinc ferrite in which the Zn^{2+} occupies the octahedral site. During the mixing of ZnO and α-Fe_2O_3 mechanically, the zinc ferrite is expected to be formed only at the surface of the particles. Hence, the XRD line corresponding to the zinc ferrite is very small. Unlike XRD, the XPS is a surface analytical tool, it probes mainly the surface of the particles. Thus, the XPS peak corresponding to the octahedral zinc is relatively more intense than the XRD line Fig. 1a.

After half an hour of heat treatment, the Zn $2p_{3/2}$ peak broadened as shown in Fig. 2b, indicating the presence of multiple phases of Zn at the surface. In the XRD

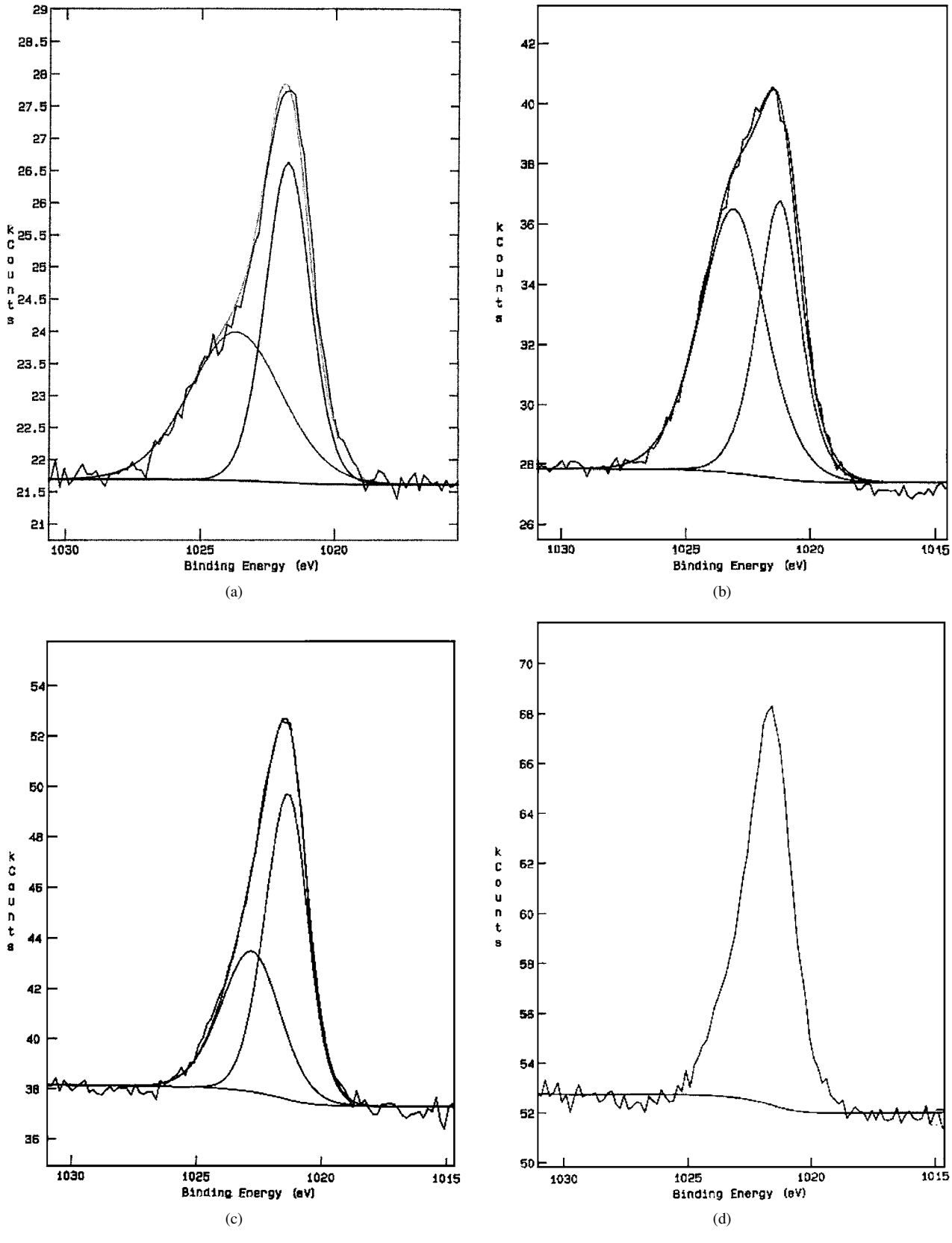

Figure 2 Zn $2p_{3/2}$ photoelectron spectra for (a) physical mixing of ZnO and Fe_2O_3, (b) annealed for 30 minutes, (c) annealed for 1 hour and (d) annealed for 3 hours. The higher energy peak indicates the presence of octahedral Zn cations at the surface due to incomplete ferrite formation.

pattern (Fig. 1b), the presence of ZnO was seen along with zinc ferrite. The peak width of Zn $2p_{3/2}$ was observed to be 3.8 eV, which was resolved into two major peaks at 1021.3 eV and 1023.2 eV with widths 2.2 and 3.0 eV as shown in Fig. 2b. The peak at 1021.3 is ascribed to the formation of zinc ferrite with the zinc atom occupying tetrahedral site. The other peak should be due to ZnO that was seen in XRD. But the width of the fitted peak was higher than that of the standard ZnO (2.2 eV) and was observed at higher binding energy than that of ZnO. Druska *et al.* [13] have reported the binding energy of Zn $2p_{3/2}$ to be around 1023.0 eV in case of $ZnTiO_3$ where zinc occupies the octahedral site. Hence we assume that the

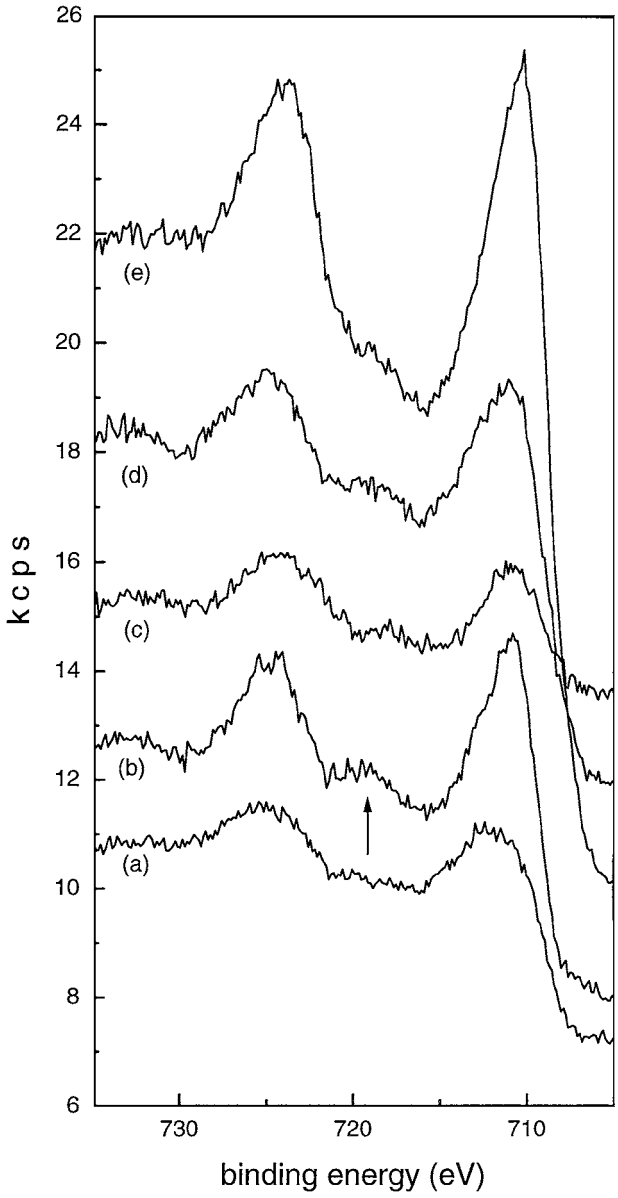

Figure 3 Fe 2p photoelectron spectra for (a) physical mixing of ZnO and Fe_2O_3, (b) annealed for 3 hours, (c) annealed for 30 minutes, (d) annealed for 1 hour and (e) magnetite. The arrow indicates the development of the satellite peak after complete removal of the Fe^{2+} by Zn^{2+}.

peak at 1023.2 eV of Zn $2p_{3/2}$ (shown in Fig. 2b) is due to the incorporation of Zn^{2+} ions at the octahedral site. So the broadness of the peak (Fig. 2b) is due to the presence of three types of Zn^{2+}, (a) Zn^{2+} in normal ferrite, (b) Zn^{2+} in oxide and (c) Zn^{2+} in octahedral site. The presence of such unstable octahedral Mn^{2+} in manganese ferrite that forms normal spinel was also reported [14]. The octahedral zinc ferrite has also been observed earlier as a result of mechanical treatment on the normal zinc ferrite [13]. The surface composition of the ferrite after half an hour of heat treatment was as follows, $Zn^{2+}O$, $(Zn^{2+})_t(Fe^{3+})_oO_4$ and $(Zn_xFe^{3+}_{(1-x)})_t(Zn^{2+}_{(1-x)}Fe^{3+}_{(1+x)})_oO_4$ ('t' for tetrahedral and 'o' for octahedral). After one hour of heating the peak width was reduced to 2.9 eV that was still broader than the width of zinc ferrite or ZnO. The deconvolution of the peak showed the presence of octahedral Zn^{2+} ions (Fig. 2c); however its intensity was reduced significantly. After three hours of heating the reaction went to completion and the peak width narrowed down to 2.2 eV (Fig. 2d). The peak position and peak width agreed well with the standard zinc ferrite sample described in Table I.

TABLE I Binding energy of Zn $2p_{3/2}$ in Zn-compounds

Materials	B.E. (eV)	FWHM (eV)	Remarks
Zn	1021.4	1.6	Solid metal.
ZnO	1021.7	2.1	Powder oxide.
$Zn_{0.33}Fe_{2.67}O_4$	1021.4	1.9	Synthesized and XPS recorded.
$Zn_{0.67}Fe_{2.33}O_4$	1021.3	2.1	Synthesized and XPS recorded after sputtering the surface.
$ZnFe_2O_4$	1021.4	2.2	Synthesized and XPS recorded.
$ZnFe_2O_4$	1021.4	2.1	XPS recorded from standard material [6].

3.1.2. Fe 2p line-shape analysis

The Fe $2p_{3/2}$ photoelectron peak is always associated with background, which makes the analysis of the peak complicated. Hence, the Fe $2p_{1/2}$ peak is taken for intensity analysis whose background is less than that of Fe $2p_{3/2}$. In Fig. 3a–e, the Fe2p photoelectron spectra for magnetite and zinc ferrite at different stages are shown. The binding energy for $Fe2p_{3/2}$ in magnetite is 710.6 eV, which matches well with the literature value [5].

After physical mixing of ZnO and Fe_2O_3, the peak width of Fe 2p was observed to be broader than the normal Fe 2p in Fe_2O_3. This implies the presence of Fe in different chemical environment in addition to Fe_2O_3 and that happened due to mechanical mixing of the powders. These results complement the shoulder in Zn 2p peak after mechanical mixing as described in Fig. 2a. After 30 minutes, the peak width reduced but a sharp peak was observed after three hours of annealing. Simultaneously, the satellite peak above 8.5 eV of the main $2p_{3/2}$ peak was observed to become very prominent after three hours (shown by arrow). It is interesting to observe that though XRD showed the complete formation in one hour, XPS showed it to be complete in three hours only as confirmed by both Fe and Zn lineshape analysis.

In magnetite, the Fe $2p_{3/2}$ peak is contributed from $2Fe^{3+}$ and $1Fe^{2+}$ ions. The binding energy values for Fe^{2+} and Fe^{3+} are 709.5 eV and 711.2 eV respectively [15]. Fe^{3+} being the dominant species in magnetite, the peak center was observed at higher binding energy side i.e. at 710.6 eV in comparison to the Fe^{2+} binding energy at 709.5 eV [15]. In case of zinc ferrite, the system does not contain any Fe^{2+}, so the binding energy was increased to 711.4 eV in comparison to Fe_3O_4. Though haematite and zinc ferrite contain Fe^{3+} type iron only, an increase in binding energy in zinc ferrite compared (711.4 eV) to that in Fe_2O_3 (711.2 eV) may be due to the change of oxygen environment of Fe in Zn ferrite.

The Fe^{2+} and Fe^{3+} photoelectron peaks are always associated with satellite peak around 6 eV and 8.5 eV respectively higher than the principal peak [15]. In Fe_3O_4, the satellite peak associated with $2p_{3/2}$ of Fe is not seen or it may be apparently absent (Fig. 3e) because of the superposition of the two satellites. No satellite was seen

in the samples annealed for 30 minutes. After one hour of heating the satellite at 8.5 eV appeared and after three hours of annealing the satellite at 8.5 eV became very distinct (arrow in Fig. 3d). This indicates the complete substitution of Fe^{2+} by Zn^{2+} ions. In pure α-Fe_2O_3 the main $2p_{1/2}$ peak to satellite peak area ratio was seen to be 2.6. In $ZnFe_2O_4$ the ratio was seen to be 2.5, which implied the complete substitution of the Fe^{2+}, by Zn^{2+} at the surface of the ferrite grains.

The zinc to iron atomic concentration ratio was also calculated for the surface of the ferrite at different stages of heat treatment using the formula (1).

$$\%\ \text{of the metal ion present in the oxide (M\%)} = \frac{I_M/S_M}{I_M/S_M + I_{M'}/S_{M'}} \quad (1)$$

I_M and $I_{M'}$ = Area of the Zn $2p_{3/2}$ and $Fe2p_{3/2}$ photoelectron peaks; S_M and $S_{M'}$ = Atomic sensitivity factors for $Zn2p_{3/2}$ and Fe $2p_{3/2}$ peaks.

After half an hour heat treatment, the surface was enriched with zinc and the zinc to iron ratio was 1.07. It reduced to 0.97 after one hour of heat treatment and after three hours the value further decreased to 0.51. Thus within three hours the reaction showed the stoichiometric formation of the ferrite.

From these observations it can be concluded directly that initially Zn diffuses to the surface of α-Fe_2O_3. A layer containing mixture of ZnO, zinc ferrite with zinc in octahedral site and normal zinc ferrite is formed over the surface of the grain. With time the Zn^{2+} ions diffuse into the α-Fe_2O_3 lattice through the ferrite layer formed on the surface and thus decreased the amount of zinc on the surface. After completion of the reaction, the Zn^{2+} on the surface is only in normal ferrite form.

3.2. Study on $Zn_xFe_{2-x}O_4$ (x = 0.3, 0.6)

The lattice parameters of the non-stoichiometric ferrites were calculated from each d spacing measurement using the formula (2),

$$a_0^2 = d^2(h^2 + k^2 + l^2) \quad (2)$$

The plot showing the variation of lattice parameter with Zn content is shown in Fig. 4, this agress well with Vegard's law. The slight deviation for $Zn_{0.67}Fe_{2.33}O_4$ from the trend may be due to improper formation of the ferrite. The increase in the lattice parameter of the zinc ferrites in comparison to the magnetite is due to the increase in the cation size at the tetrahedral interstices. The Fe^{3+} ions at tetrahedral site in the inverse spinel magnetite have lower ionic radius than Zn^{2+} in tetrahedral site in normal Zn ferrite.

In Fig. 5, Zn $2p_{3/2}$ photoelectron spectra from different zinc ferrites are shown. The binding energy of Zn $2p_{3/2}$ from ZnO agrees well with the literature value [12]. In Table I, the binding energy values are shown. In zinc ferrite, the binding energy was observed to be 1021.4 eV and was slightly lower than the ZnO binding energy. Similar decrease in binding energy has been seen in the case of Mn $2p_{3/2}$ when it is placed in a spinel lattice from the MnO [4].

The chemical shift of a photoelectron peak is primarily due to two factors, (i) the final state effect of

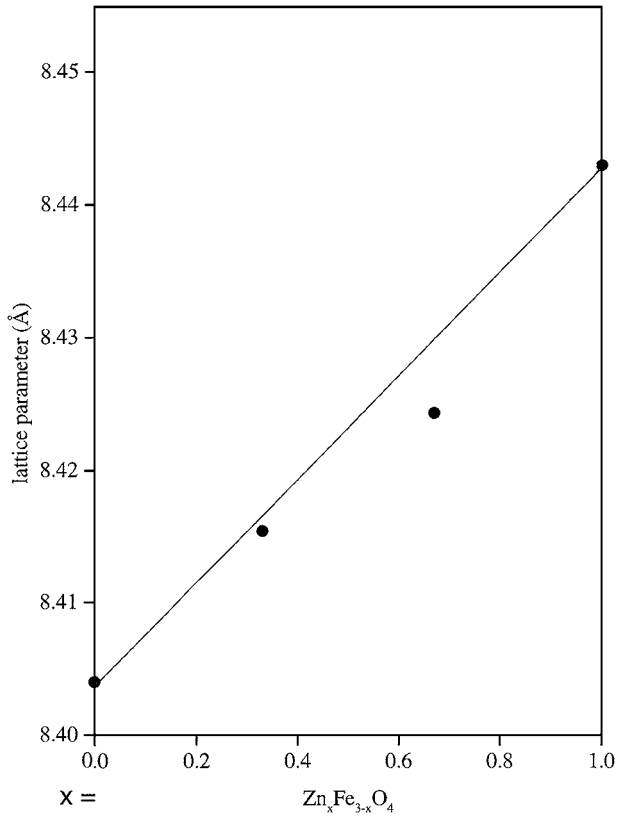

Figure 4 Lattice parameters calculated from X-ray diffraction patterns are plotted as a function of Zn content in the spinel series $Zn_xFe_{3-x}O_4$.

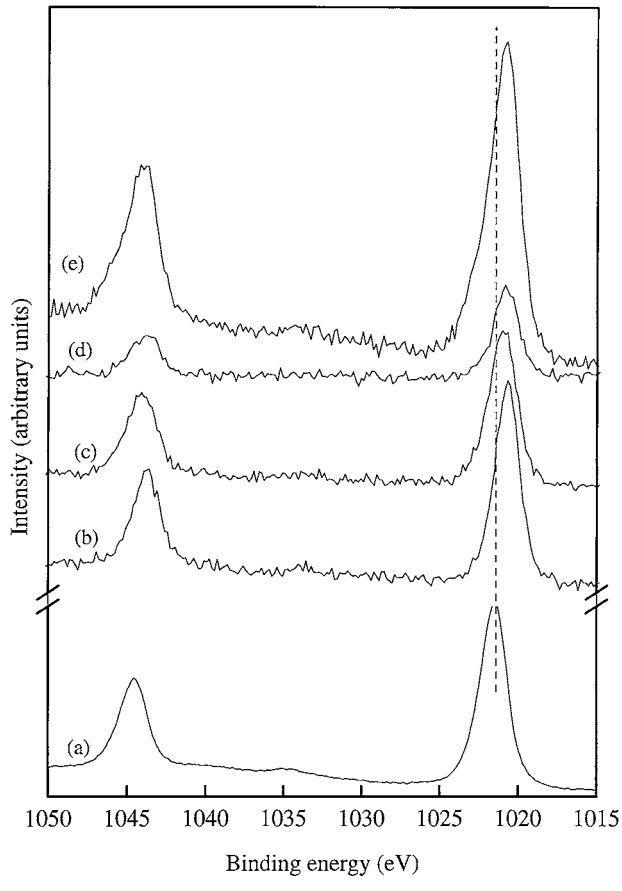

Figure 5 Zn 2p photoelectron spectra for (a) ZnO, (b) standard $ZnFe_2O_4$, (c) $Zn_{0.67}Fe_{2.33}O_4$, (c) $Zn_{0.33}Fe_{2.67}O_4$ and (e) $ZnFe_2O_4$ prepared.

relaxation and (ii) the initial state effect due to the changed electronic environment of the atom. The shift due to electronic environment may be called as the true binding energy shift that appears due to valence band redistribution after the reaction. The chemical shift of Zn $2p_{3/2}$ electrons due to electronic environment will be the same for both oxide and normal zinc ferrite. In the process of ferrite formation Zn repositions itself to the tetrahedral site of the spinel and thus the final state effect causes a decrease in the binding energy.

In the non-stoichiometric ferrite viz. $Zn_{0.33}Fe_{2.67}O_4$, the Zn/Fe atomic concentration ratio obtained from XPS peak intensity was 0.1 that is well matching with the formula. For $Zn_{0.67}Fe_{2.33}O_4$ the ratio was three times more than the expected value. This shows that Zn was enriched on the surface in the later case.

To probe the reason of zinc enrichment on the surface, the FWHM of the $Zn2p_{3/2}$ peak has been measured for both cases. In case of $Zn_{0.33}$ ferrite, the FWHM was observed to be 2.2 eV, well matching with the standard zinc ferrite value. But in $Zn_{0.66}$ ferrite the FWHM was 2.7 eV that is significantly higher than the standard value. The broader FWHM may be due to the presence of trace of unreacted ZnO that is not detected by XRD. In Fig. 6, the change in Zn/Fe atomic concentration ratio is shown with the sputtering time. It is seen that the ratio is approaching to the lower value after several layers. The sputtering beam current was kept at 1.5 μA, and the sputtering rate was approximately 2 Å/minute. The FWHM was also seen to change from 2.7 eV gradually and reached 2.1 eV after 12 Å. The change in the FWHM may be due to the removal of the surface Zn-O layer that caused the enrichment of zinc at the surface in $Zn_{0.67}$ ferrite case. The enrichment of Zn at surface might have reduced Zn content in bulk. So in XRD the material was seen as less zinc content than the expected and that caused a deviation of its lattice parameter from the Vegard's plot (Fig. 1).

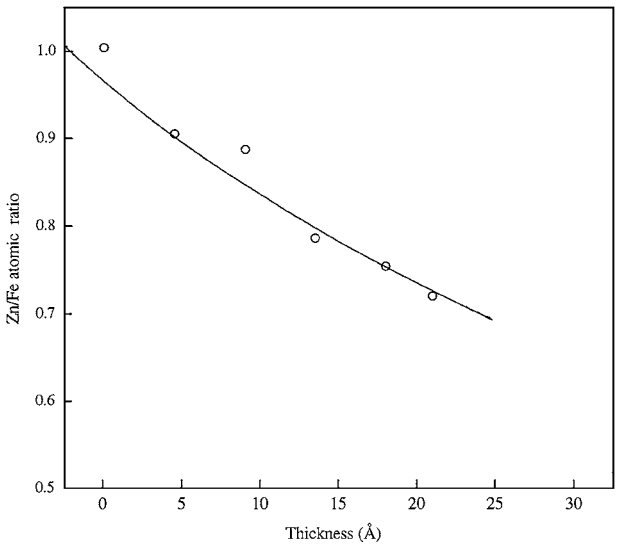

Figure 6 Surface sputtering of $Zn_{0.67}Fe_{2.33}O_4$ by Ar ion (beam current 1.5 μA), shows the gradual decrease of Zn content at different depth of the grain surface. The Zn/Fe atomic ratio approaches a lower value.

4. Conclusions

1. The formation of zinc ferrite by the solid state method and its characterization by XRD and XPS are undertaken. The binding energy of the Zn $2p_{3/2}$ in zinc ferrite was observed to be lower than that in ZnO. The lowering of the binding energy was explained in terms of atomic environment of the Zn cations.

2. The growth of the ferrite at the surface was observed by XPS. Due to heat treatment, ZnO and Fe_2O_3 mixture reacts to form inverse zinc ferrite that is in equilibrium with normal zinc ferrite. With longer heat treatment normal ferrite is obtained.

3. During the formation of non-stoichiometric $Zn_{0.67}Fe_{2.33}O_4$, the surface of the ferrite was enriched with Zn. The desired ratio was observed after sputtering away few atomic layers of the ferrites.

Acknowledgement

The authors thank Dr. Tadao Kanzaki of Iwaki Meisei University, Japan for supplying the standard $ZnFe_2O_4$ samples. They thank Mr. E. Prabhu and Dr. V. Jayaraman for providing sample preparation facility. One of the authors (AAMP) thanks CSIR (India) for the award of Senior Research Fellowship to him.

References

1. M. HAGINUMA, S. ONO, K. TAKAMORI, K. TAKEDA, K. TACHIBANA and K. ISHIGURE, *Water Chemistry of Nuclear Reactor Systems, BNES* **7** (1996) 128.
2. J. A. SAWICKI and H. A. ALLSOP, *J. Nucl. Maters.* **240** (1996) 22.
3. I. KAUR and W. GUST, "Grain and Interphase Boundary Diffusion" (Ziegler Press, Stuttgart, 1989).
4. G. C. ALLEN, S. J. HARRIS and J. A. JUSTON, *Appl. Surf. Sci.* **37** (1989) 111.
5. G. C. ALLEN and K. R. HALLAM, *ibid.* **93** (1996) 25.
6. T. KANZAKI, K. KITAYAMA and K. SHIMOKOSHI, *J. Amer. Ceram. Soc.* **76** (1993) 1491.
7. D. K. ZIA and C. A. PICKLES, *Metall. Materls. Trans B* **28B** (1997) 671.
8. I. HALIKIA and E. MILONA, *Canadian Metall. Quarterly* **33** (1994) 99.
9. A. A. M. PRINCE, S. VELMURUGAN, A. K. TYAGI, S. V. NARASIMHAN, P. S. RAGHAVAN and R. GOPALAN, JAIF International Conference on Water Chemistry in Nuclear Power Plants (1998) 747.
10. D. K. SARKAR, S. BERA, S. V. NARASIMHAN, S. DHARA, K. G. M. NAIR and S.C. CHOWDHURY, *Appl. Surf. Sci.* **120** (1997) 159.
11. V. SEPELAK, U. STEINIKE, D. C. UECKER, S. WIβMANN and K.D. BECKER, *J. Solid State Chem.* **135** (1998) 52.
12. C. D. WAGNER, W. M. RIGGS, L. E. DAVIS, J. F. MOULDER and G. E. MUILENBERG, "Handbook of XPS" (PE Corporation, USA, 1979).
13. P. DRUSKA, U. STEINIKE and V. SEPELAK, *J. Solid State Chem.* **146** (1999) 13.
14. J. M. HASTINGS and L. M. CORLISS, *Phys. Rev.* **104** (1956) 328.
15. WANDELT, *Surf. Sci. Reports* **2**(1) (1982) 1.

Received 20 October 2000
and accepted 3 August 2001